Photodetectors based on two dimensional materials*

Lou Zheng(娄正)[1], Liang Zhongzhu(梁中翥)[2], and Shen Guozhen(沈国震)[1,†]

[1]Institute of Semiconductors, Chinese Academy of Sciences, Beijing 100083, China
[2]State Key Laboratory of Applied Optics, Changchun Institute of Optics, Fine Mechanics and Physics, Chinese Academy of Sciences, Changchun 130033, China

Abstract: Two-dimensional (2D) materials with unique properties have received a great deal of attention in recent years. This family of materials has rapidly established themselves as intriguing building blocks for versatile nanoelectronic devices that offer promising potential for use in next generation optoelectronics, such as photodetectors. Furthermore, their optoelectronic performance can be adjusted by varying the number of layers. They have demonstrated excellent light absorption, enabling ultrafast and ultrasensitive detection of light in photodetectors, especially in their single-layer structure. Moreover, due to their atomic thickness, outstanding mechanical flexibility, and large breaking strength, these materials have been of great interest for use in flexible devices and strain engineering. Toward that end, several kinds of photodetectors based on 2D materials have been reported. Here, we present a review of the state-of-the-art in photodetectors based on graphene and other 2D materials, such as the graphene, transition metal dichalcogenides, and so on.

Key words: 2D materials; graphene; photodetector
DOI: 10.1088/1674-4926/37/9/091001 **PACS:** 85.60.Gz **EEACC:** 2520

1. Introduction

Photodetectors which can convert the light into electrical signals are the key factors of many applications that affect our daily life[1−5]. Their applications, such as optical communications, video imaging, security, motion detection, and night-vision have been very mature due to the development of integration technologies, large-scale production, and good performance materials. As their range has grown and their applications have diversified, the requirements for photodetectors have also increased. Following the successful preparation of graphene a few years ago, two-dimensional (2D) materials have gained widespread attention in the field of electronics and optoelectronics[6−8].

Graphene is the first widely studied material with a true 2D nature and it provides some unique advantages when compared with other materials[9−13]. Different kinds of optoelectronic devices based on graphene have been developed, including ultrafast lasers, optical modulators, photovoltaic modules and transparent electrodes[14−17]. Among these, considerable developments have been devoted to design graphene based photodetectors which have distinct characteristics. First, they have unique band structures. Such gapless materials can absorb light with a very wide spectral range to generate charge carriers. So graphene photodetectors include the ultraviolet, visible, short-, near-, mid- and far-infrared and terahertz spectral regimes. Moreover, graphene also shows high mobility, low dissipation rates, tunable optical properties, wavelength-independent absorption and ultrafast carrier dynamics[18−24]. Such high carrier mobility can fast convert the photons or plasmons to electrical signals. Over the past few years, many of the unique capabilities and characteristics of graphene based photodetection systems have been widely studied and several applications have been addressed. Some graphene photodetectors have already achieved the commercial criterion. More importantly, graphene is compatible with the silicon-based devices that are used in electronics and photonics, which means that they have great promise in developing low-cost and large-scale integration into optoelectronic devices[25−27].

Graphene is not the only 2D crystal which has been investigated for photodetectors[28,29]. There are other layered materials that keep their stability in monolayers and which are complementary to those of graphene. For example, transition metal dichalcogenides (TMDs) and oxides (TMOs) have a layered structure. Covalent bonds hold the atoms together within each layer and van der Waals interactions hold different layers together[30]. Due to their mechanical flexibility, transparency, and easy processing, TMDs can show additional advantages for use in photodetectors compared with classical semiconductors. Furthermore, TMDs can also detect light at different wavelengths by tuning the bandgap by varying the number of layers[31−33]. These characteristics can complement graphene based photodetectors. Graphene is often used in ultrafast and broadband technologies, whereas TMDs have the advantages of strong electroluminescence and light absorption[34−36]. Hence, with the large availability of empty states, an electron–hole pair can probably be increasingly excited with a photon that has an energy close to the bandgap. Moreover, 2D materials have also shown large strain before rupture and excellent elastic modulus. The optical and electronic properties of these materials can be strongly affected by large strains[37]. Therefore, their optical properties can be tuned by

* Project supported by the National Natural Science Foundation of China (Nos. 61377033, 61574132, 61504136) and the State Key Laboratory of Applied Optics, Changchun Institute of Optics, Fine Mechanics and Physics, Chinese Academy of Sciences.
† Corresponding author. Email: gzshen@semi.ac.cn
Received 30 July 2016

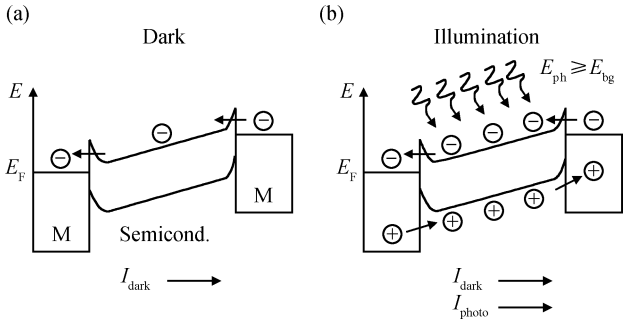

Figure 1. Schematic of the photoconductive effect. (a) In the dark. (b) Under illumination[38].

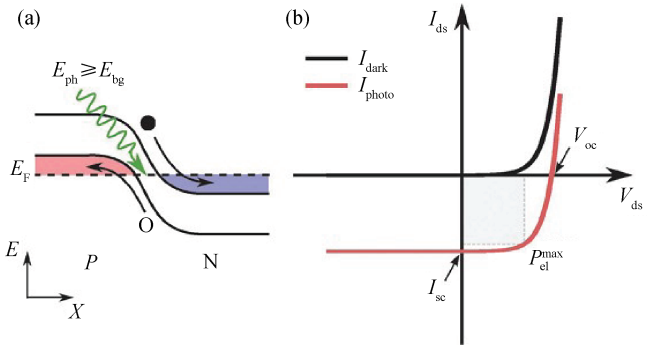

Figure 2. (Color online) Schematic of the photovoltaic effect. (a) Band alignment in a PN junction. (b) I–V curves in the dark and under illumination[38].

strain-engineering. Novel device architectures, such as wearable and bendable devices with novel functionalities, can be developed by introducing 2D materials.

In this review, we present a comprehensive summary of 2D materials based photodetectors that have been developed in the past. As there are many comprehensive reviews focusing on 2D material synthesis and assembly, this field will not be reviewed in this article. The mechanisms of the photodetector are first discussed in detail in this review, including photoconductive effect, photovoltaic effect, and photo-thermoelectric effect. Next, the different 2D materials used in photodetectors are introduced, followed by some predictions for the future direction of 2D materials based PDs.

2. The physical mechanisms that are used in photodetectors

This section introduces the physical mechanisms that are used in photodetectors. The important factor in the application of the photodetector and other optoelectronic devices is the conversion of photons to electrical signals. Different mechanisms used in photodetectors have been reported, including the photoconductive effect, photovoltaic effect and photothermoelectric effect.

2.1. Photoconductive effect

The photoconductive effect is based on the generation of free carriers by photon absorption, which can increase the electrical conductance of the semiconductor, as shown in Figure 1[38–41]. When the device was under an applied bias and without illumination (Figure 1(a)), there was a small current between the two electrodes (I_{dark}). When the device was exposed to light, photons with a higher energy than the bandgap can generate electron–hole pairs that are separated by the applied voltage (Figure 1(b)). Such free electronic and holes drift in two different directions between the metal leads, leading to an increase of the current (I_{photo}). The photogenerated current increased the conductivity of the device.

It is instructive to study the large difference between the electron and hole transit time ($\tau_{transit}$), due to the large difference between the electron and hole mobilities[40]:

$$\tau_{transit} = L^2/(\mu V_{ds}). \quad (1)$$

where L, V_{ds} and μ correspond to the length of the transistor channel, the source–drain voltage and the charge carrier mobility, respectively. It is worth noting that if the electron mobility is much higher than the hole mobility, this results in a faster channel crossing of the photogenerated current. Many electrons can take part in the photocurrent before hole extraction or recombination, which generates the photoconductive gain (G). In fact, this means that a single photon can extract more electrons, which leads to a quantum efficiency larger than one. The photoconductive gain is the ratio of the photogenerated carrier lifetime ($\tau_{photocarriers}$) and the transit time[40]:

$$G = \tau_{photocarriers}/\tau_{transit} = \tau_{photocarriers} V_{ds}\mu/L^2, \quad (2)$$

Therefore, large G can be yielded by a large mismatch in the electron/hole and large photocarriers.

2.2. Photovoltaic effect

In the photovoltaic (PV) effect, PV photocurrent generation relies upon the photogenerated electron–hole (e–h) pairs separated by an internal electric field. Some interface can build the internal electric field, such as the Schottky barrier or a PN junction, as shown in Figure 2(a). Under these circumstances, the detectors exhibit nonlinear I–V properties in the dark. As the PN junctions formed, I_{ds} is exponential with the V_{ds} as $I_{ds} \propto \exp V_{ds} - 1$. On the other hand, before the junction breakdown, the reverse current is negligible[42]. When the device was under illumination without external voltage, the photogenerated e–h pairs can be separated by the internal electric field leading to a large photocurrent. The open circuit voltage can be generated due to the accumulation of carriers of opposite polarities that keep the circuit open. When the device was under illumination and reverse bias, the photogenerated carriers are wiped out in opposite directions, leading to the increasing magnitude of the reverse current. Compared with the photoconductive effect, the energy of the photons can be converted to electrical energy by the photovoltaic effect.

Figure 2(b) shows the I–V properties of the PN junction under illumination and in the dark. Most of the PV effect based photodetectors are PN diodes. They always work without bias voltage or under reverse bias voltage. In the zero voltage, there is the lowest dark current, which improves the detectivity of the photodetector. But, the photo responsivity is smaller than the device which works at the photoconducting mechanism because of the deficiency of the internal gain. The reverse-bias

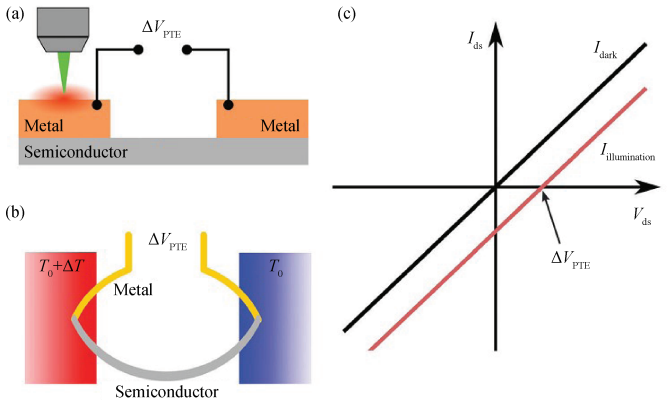

Figure 3. (Color online) Schematic of the photo-thermoelectric effect. (a) Schematic of a field-effect transistor. (b) Thermal circuit corresponding to the device depicted in (a). (c) I_{ds}–V_{ds} characteristics in the dark and under illumination[38].

operation can reduce the junction capacitance, which increases the speed of the photodiode. This mechanism can offer great internal gain, which means that the device can detect light with extremely low power.

2.3. Photo-thermoelectric effect

In the photo-thermoelectric effect (PTE) a light-induced heating leads to a temperature gradient through a semiconductor channel. Hence, there is a temperature difference ΔT between the two ends of the semiconductor channel. Due to the Seebeck effect (Figure 3), the ΔT can convert into a voltage difference ΔV. Via the Seebeck coefficient (S), the magnitude of ΔV and the temperature gradient are linearly proportional[43]:

$$\Delta V = S \cdot \Delta T. \tag{3}$$

Localized illumination with a laser spot that is much smaller than those of the testing photodetector can generate a heat gradient. In addition, a strong difference absorption in an unusual part of the photodetector under the entire illumination can also generate a heat gradient.

At zero bias voltage, a current can be driven by a voltage difference which is generated by a temperature gradient through PTE. As shown in Figure 3, a model can be built where two junctions between the contact semiconductor and the metal channel are formed as a focused laser spot illuminates the device. For instance, a steady-state ΔT between two junctions was kept by a focused illumination on the electrical contacts, resulting in a voltage difference (ΔV_{PTE}).

$$\Delta V_{PTE} = (S_{semiconductor} - S_{metal}) \cdot \Delta T \approx S_{semiconductor} \cdot \Delta T. \tag{4}$$

In the equipment, because the Seebeck coefficients of pure metals are much smaller than those of the semiconductors, that we can neglect the term of $S_{metal} \cdot \Delta T$. Here, ΔT can be calculated by measuring with on-chip thermometers, or finite element simulations[44–46]. So, as ΔT is confirmed, the Seebeck coefficient of the semiconductor material can be easily estimated. The selectivity of the electrode materials is very important to drive the current through the device, which needs the electrode materials to form ohmic contacts to the semiconductor. So, if a uniform semiconducting channel is illuminated without an external bias voltage, there is no current will flow and the thermal gradients can be negligible.

3. Graphene photodetector

Graphene can absorb photons with a banding energy from ultraviolet to mid-infrared wavelengths, due to the interband transitions of carriers and zero bandgap[47, 48]. Unfortunately, due to its innate thinness, monolayer graphene has a small optical absorption and this has limited the photoresponsivity of the photodetectors based on graphene. The first graphene photodetector exhibited a 500 GHz bandwidth, and a 0.5 mA/W photoresponsivity[49]. This device has a short effective region of 0.2 μm. As shown in Figure 4(a), a metal–graphene–metal (MGM) photodetector which has asymmetric electrodes has been investigated to extend the operation region, with an external photoresponsivity of 6.1 mA/W[50].

Photodetectors based on graphene have some important advantages, such as high speed, ultra-broadband, and compatibility to circuits. But, compared with the traditional semiconductors, graphene photodetectors have lower photoresponsivity, which remains a major drawback. In recent years, some methods have been investigated to improve the optical absorption of graphene photodetectors. For example, with the introduction of plasmonic nanostructures, the device can concentrate light utilizing plasmonic resonances, leading to a great improvement in the local electric field[51, 52]. Such plasmonic nanostructures can not only have a large enhancement in quantum efficiency but they can also achieve multicolor detection through the wavelength-dependence[53]. As shown in Figure 4(b), plasmonic nano-antennas sandwiched between the two graphene monolayers can achieve a quantum efficiency of up to 20%. But there is also a significant drawback of this type device: the working wavelength of the photodetectors can be determined by the resonance of nanostructures in these systems, typically resulting in a reduced operation bandwidth.

Another method is to integrate quantum dots with graphene to improve the photoresponsivity of graphene based photodetectors. Konstantatos and his group[54] introduced colloidal quantum dots to develop a hybrid photodetector with a photoresponsivity of $\sim 10^7$ A/W and ultrahigh photodetection gain ($\sim 10^8$). The effect of the quantum dots helps the photogenerated carriers to arrive at the graphene sheets while trapping all of the opposite carriers, leading to a field-effect doping phenomenon. Photodetectors based on graphene–PbS quantum dots have also been fabricated on a flexible substrate, which has a great photoresponsivity of 10^7 A/W[55]. Some drawbacks have also appeared in graphene-quantum dot photodetectors, such as low operational speed and working bandwidth, because in these devices this is mainly determined by the quantum dot.

Furthermore, another useful method is to integrate graphene with microcavity to increase photoresponse[56–59]. As shown in Figure 4(c), in the first graphene-cavity photodetector Fabry–Pérot microcavities were formed by two opposite mirrors, which have a 20-fold improvement of photocurrent under illumination. Such a useful method can improve the photoresponse but it also narrows the bandwidth.

At last, coupling with various waveguides can make graphene photodetectors that have a great performance[60–64]. These photodetectors have high speed, high efficiency, ultra-

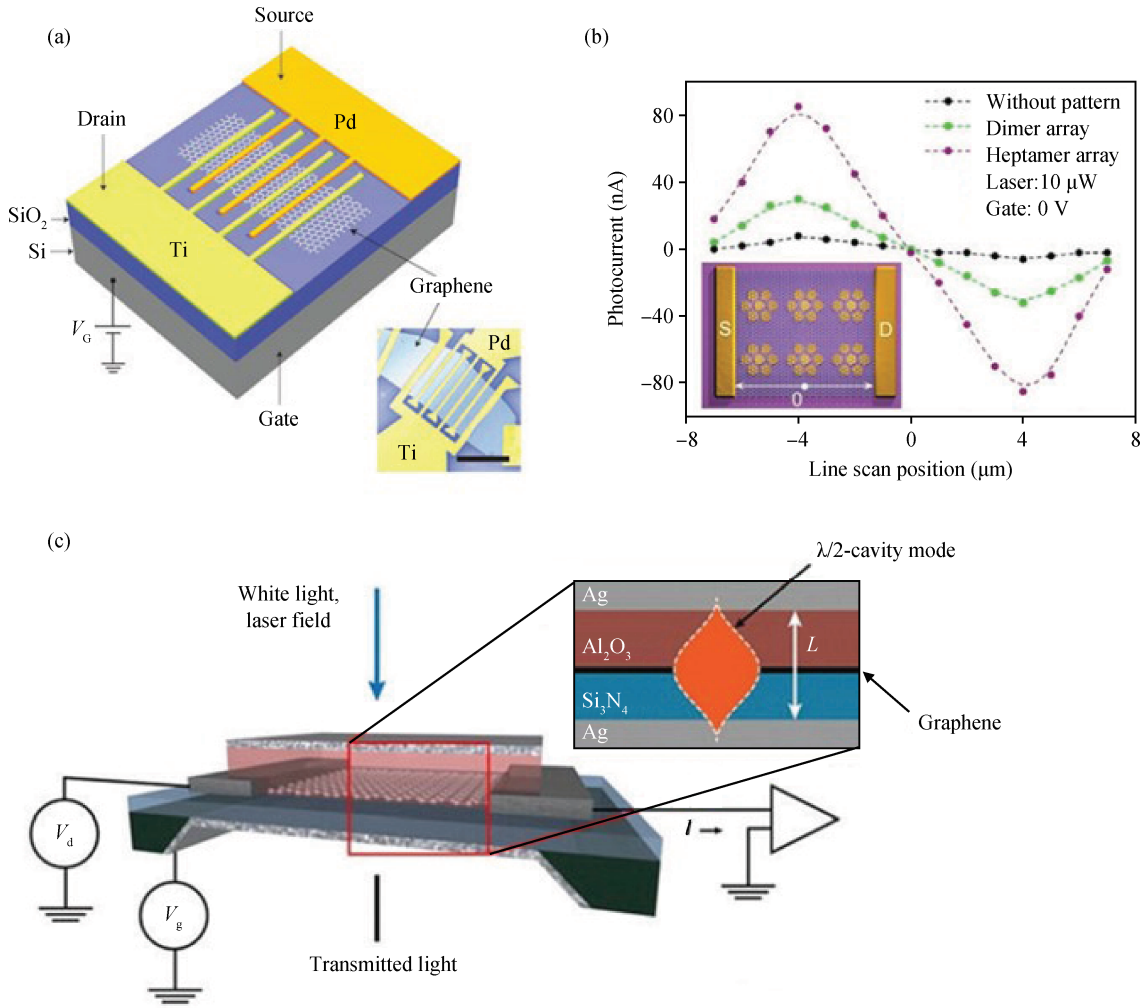

Figure 4. (Color online) (a) Schematic of the metal–graphene–metal photodetector[50]. (b) Geometry-dependent photoresponse in antenna-graphene sandwich structure[53]. (c) Schematic of the graphene-microcavity photodetector[56].

wide bandwidth, and high photoresponsivity. In graphene-waveguide systems, batt-coupling or evanescent coupling can both convey light to graphene. Although this will inevitably result in a larger device dimension when integrated with a waveguide, graphene-waveguide photodetectors with wide adsorption bandwidth give them an advantage over traditional photodetectors[63].

4. Transition metal (Mo, W) dichalcogenides photodetectors

Few-layer transition metal dichalcogenides (TMDCs) based photodetectors have larger photoresponsivity compared with the graphene based photodetectors. But these devices always work at the visible region. Various 2D TMDCs have been used for high performance photodetectors, such as $ReSe_2$, WS_2, MoS_2, and so on[65]. Due to their mechanical flexibility and easy processing, TMDCs can provide additional advantages in the field of optoelectronics compared with classical direct-bandgap semiconductors.

Mechanical exfoliation has opened up a new method to produce synthesized of FETs based on single-layer or few-layer TMDCs, and it can also help us to study their optoelectronic properties.

4.1. Molybdenum disulphide

As one of the most studied semiconducting TMDCs, MoS_2 has a large and direct bandgap of 1.8 eV, high mobility of above 100 $cm^2/(V{\cdot}s)$[66–69]. Moreover, its remarkable mechanical characteristics make single and few-layer MoS_2 a potential material for use in optoelectronic and flexible devices[70–77].

MoS_2 based photodetectors are always in the form of a photo-FET. Firstly, Yin and his group[78] developed a single-layer MoS_2 based photo-FET which can measure 750 nm light, with a photoresponsivity of 7.5 mA/W and a response time of 50 ms, as shown in Figure 5(a). A similar study has also been investigated by Lopez-Sanchez and his group[79], who made phototransistors based on monolayer MoS_2 with high sensitivity. The device can arrive at a responsivity of 880 A/W with a cut-off wavelength of 680 nm as shown in Figure 5(b). In addition, the photocurrent rises as the light power increased, as shown in Figure 5(c). The response time can be reduced from 4 to 0.6 s with the help of gate pulse. More importantly the photodetector shows a high NEP value of 1.8×10^{15} $WHz^{1/2}$. Such a low NEP was attributed to which efficient field-effect tenability and 1.8 eV bandgap was in used in the monolayer

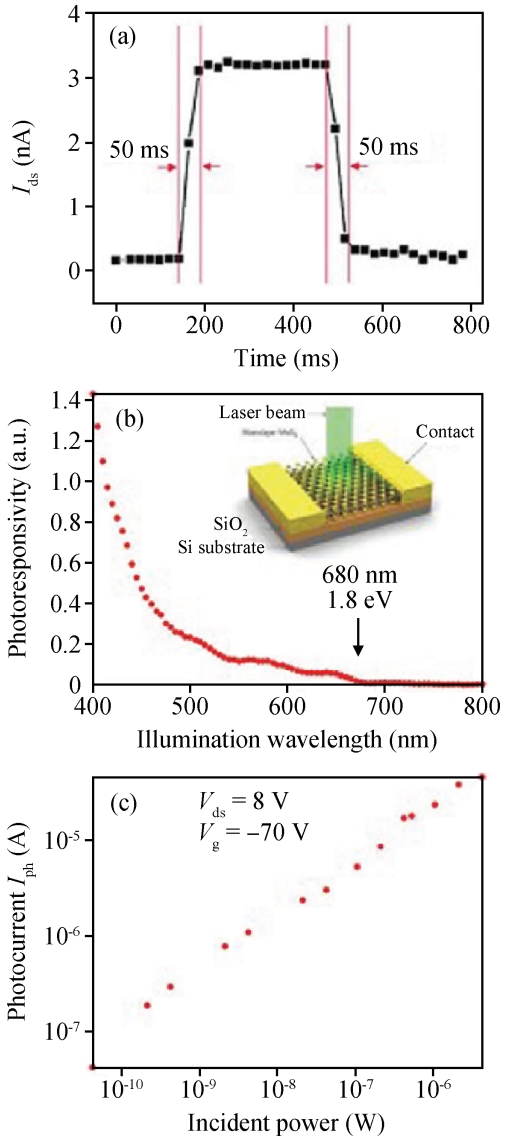

Figure 5. (Color online) (a) Time response of the device[78]. (b) Photoresponsivity as a function of illumination wavelength. (c) Photocurrent as a function of incident optical power[79].

MoS_2, leading to the low dark current in electron depletion.

Recently, Zhang *et al.*[77] grew single-layer MoS_2 by the chemical vapor deposition (CVD) method. Their device shows the different responsivities in vacuum and in air, corresponding 2200 A/W in vacuum and 780 A/W in air, respectively. This implies that the environment has a great influence on both the electronic and the optoelectronic properties. Adsorbates are an important factor in the performance of layered materials, due to the large surface-to-volume ratio[80–83]. As recombination centers, the charged adsorbates suppress the lifetime of trapped carriers, which will reduce the photoresponse. Similar results were given by Perea-Lopez *et al.*[84], which are five orders of magnitude lower.

MoS_2 with different synthesis methods like exfoliated and CVD-grown all exhibit high responsivity, fast response speed from ms-to-s and sub-linear change with incident optical power. All of these properties arise because the photogeneration mechanism with trap states plays an important role. In particular, the photocurrent generation mechanism can conclude two keys, one is the photoconductance, the other is the photogating, which has been reported by Furchi[85]. In his study, Furchi points to the relationship of the photoresponse of single and bilayer MoS_2 with the modulation frequency of the optical excitation and different incident optical power.

Besides single-layer MoS_2, multilayer MoS_2 photodetectors have unique properties, such as bandgap reduction, which can extend the detection range, leading to a larger absorption because of the increasing thickness, but they have a lower responsivity than single-layer photodetectors. The reduction in responsivity is caused by the indirect bandgap[86]. The trap states still dominate the photodetection mechanism in multilayer MoS_2. These results show that single- and few-layer MoS_2 based biased photodetectors usually have a large responsivity, which indicates the high photogain due to the long lifetime of the photogenerated carriers, boosted by trap states.

4.2. Molybdenum diselenide

Recently, several groups have grown Molybdenum diselenide ($MoSe_2$) via CVD techniques, synthesizing large area continuous films or triangular flakes on different substrates[87–91]. These photo-FETs are fabricated by transferring the patterned electrodes on the as-grown films or flakes to an oxidized silicon wafer. Photodetectors based on $MoSe_2$ grown by CVD exhibit high responsivity between 0.26[88] and 13 mA/W[92]. In recent years, a 20 nm thick $MoSe_2$ exfoliated flake based photodetector was transferred on Ti electrodes, showing a responsivity 10^6 up to 97.1 A/W[93]. All of the studied $MoSe_2$ devices show a fast response speed, within a few tens of milliseconds.

4.3. Tungsten disulfide

As an important type of 2D materials, tungsten disulfide (WS_2) has also been investigated for use in photodetectors[94, 95]. Recently, Huo and his group[95] found that the photoresponse has a considerable influence on the gaseous environment with the performing measurements. At low excitation powers, the photoresponsivity of the device ranges from 13 A/W in vacuum to 884 A/W in NH_3 atmosphere. The increase in the NH_3 atmosphere can be explained by the charge transferring from the absorbed molecules to the WS_2 flake, which further impacts the doping level. The lifetime of the photogenerated carriers can be extended due to the charge transfer, resulting in an improvement in the responsivity. Several groups have fabricated photodetectors based on MoS_2, $MoSe_2$ and WS_2 with good sensing performance.

4.4. Tungsten diselenide

Besides the MoS_2, $MoSe_2$ and WS_2, tungsten diselenide (WSe_2) can also be used as a sensing material for photodetectors. Zhang and his group[96] reported the influence between the WSe_2 and the metal electrodes on the photoresponse. As the electrodes were Pd or Ti, the responsivity reaches 180 and 30 A/W, respectively. In contrast, the response speed of the devices with Ti electrodes is several magnitudes faster than that of the Pd electrodes. This interesting phenomenon is due to the large difference in SBs induced by Ti and Pd, which is one of

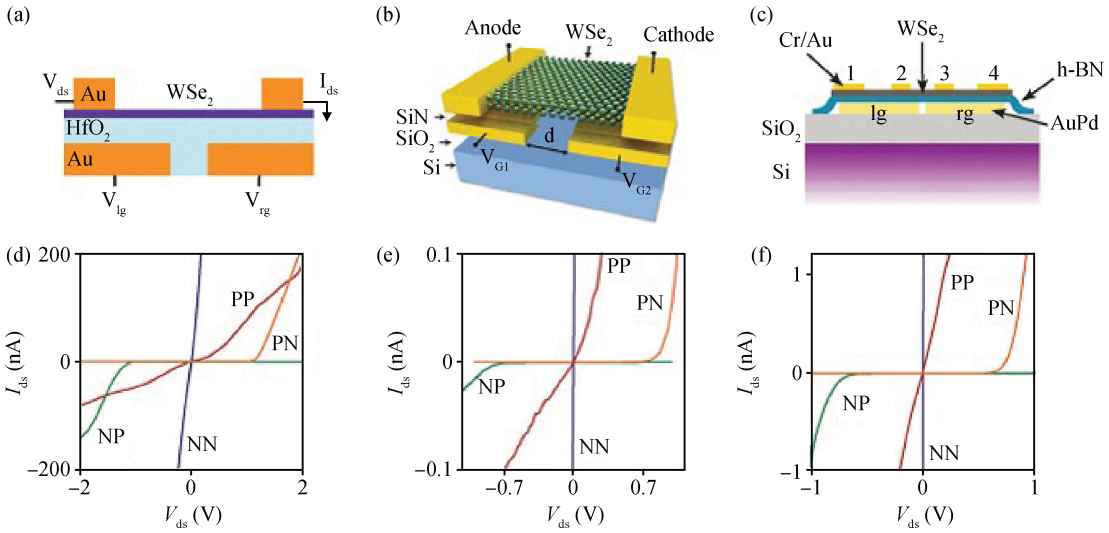

Figure 6. (Color online) (a–c) Device schematics. (d–f) I_{ds}–V_{ds} characteristics measured in different gate configurations. (a) and (d) from Reference [101]. (b) and (e) from Reference [102]. (c) and (f) from Reference [103].

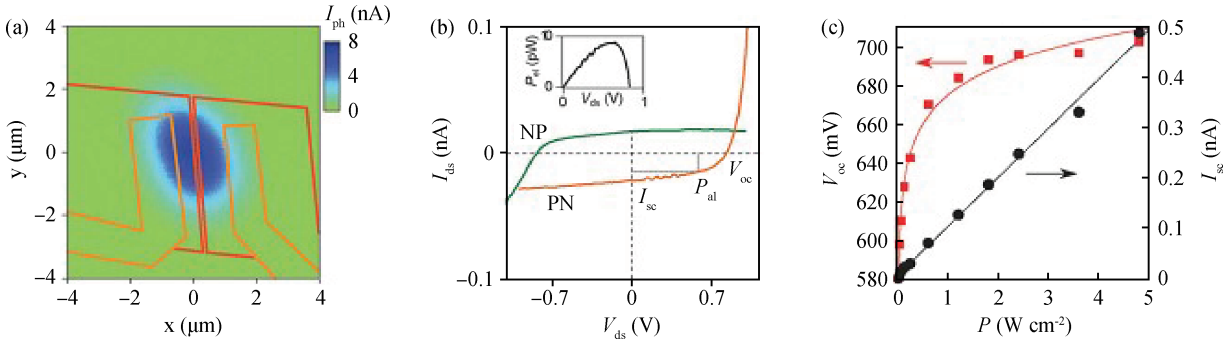

Figure 7. (Color online) (a) SPCM map of the photocurrent of the device from Reference [101]. (b) I_{ds}–V_{ds} characteristics measured in PN and NP configuration under white light illumination from Reference [102]. (c) V_{∞} and I_{sc} as a function of excitation power from Reference [103].

the most important factors for 2D materials based photodetectors.

Compared with the WS_2, $MoSe_2$ and MoS_2, WSe_2 based devices have demonstrated ambipolar transport by electrostatic gating[97–99]. Use of this property, single-layer WSe_2 can be fabricated as locally-gated PN junctions[100]. In this section, the PN junctions in recent studies will be reviewed. Figures 6(a)–6(c) show the schematics of devices with the locally-gated PN junction[101–103]. The as-fabricated PN junctions have three parts, which are the single-layer WSe_2, the source–drain and gate electrodes and the dielectric, which can be a layered hBN material or conventional (Si_3N_4 or HfO_2). The single-layer WSe_2 contacted with Cr/Au electrodes exhibited low Schottky barriers. The charge carrier density and type in the WSe_2 channel can be effectively controlled, which can give rise to a PN junction. I_{ds}–V_{ds} characteristics shown in Figures 6(d)–6(f) illustrate the effect of the local gates on the electrical transport. The I_{ds}–V_{ds} properties can be regulated from metallic to rectifying with opposite direction by controlling the gate configuration. The I_{ds}–V_{ds} properties in different configurations show a low saturation current and a high resistance, in three independent studies, implying nearly ideal diode behavior due to the large bandgap of monolayer WSe_2. This property can reduce parallel pathways for current flow, such as field emission and thermally-activated carriers. The photodetectors also have larger resistivity in the PP configuration than in the NN configuration. This behavior may imply a bigger SB for hole injection derived from the Cr/Au contacts. These studies show that different magnitudes of I_{ds} may be due to the differences of the device fabrication, measurement conditions or gate-induced carrier density.

The response to light detection of such locally gated PN junctions has been studied. Figure 7(a) exhibits a false-color map of the photocurrent on Figure 6(a) shown device in NP gate configuration. Although the long wavelength limited the spatial resolution, the PN junction electric field indeed dominated the photocurrent generation at the depletion region. For PN and NP configuration, the I_{ds}–V_{ds} under illumination is shown in Figure 7(b). Both of the curves show similar properties: as the reverse current increases, it gives rise to an open-circuit voltage and short-circuit current. These behaviors clearly point out that the photovoltaic effect can drive the photocurrent generation, as expected in a PN junction. The power intensity of the light is from tens of pW to hundreds of pW. The open-circuit voltage and short-circuit current for increasing excitation power are shown in Figure 7(c). All of the studies show linear variation between the short-circuit current and open-circuit voltage, indicating the ideal diode behavior. The

NEP of the locally gated single-layer WSe_2 based photodetectors may be much lower in photovoltaic operation because of the rather small dark current. The response speed is about 10 ms, which can also be regulated by the reverse bias.

5. Other 2D material photodetectors

Besides the graphene and chalcogenides that we discussed previously, some indium-chalcogenide or gallium-chalcogenide compounds also have a great potential for application in photodetectors[104−109]. With similar properties, the materials with layered structure are bound up with van der Waals forces. But, there are obvious differences between the structure of single layer and single-layered TMDCs. As the stoichiometry is 1 : 1, take GaS as example, the atoms arrangement in each layer is S–Ga–Ga–S. The atoms are arranged in a direction perpendicular, like the honeycomb lattice of graphene[107]. The bandgap of GaS and GaSe is different because of the dominant indirect transitions, in which for GaS the indirect and direct are 2.59 and 3.05 eV, respectively, for GaSe, the indirect and direct are 2.11 and 2.13 eV, respectively[110−114]. There is little difference of GaTe with the bandgap of 1.7 eV, resulting in a dominant direct transition[115]. In_2Se_3 with more complex layer structure has influenced their electrical properties by a variety of structural phases. For α-phase, it is direct bandgap (1.3 eV)[116−118]. These materials have been transferred on regular substrates or on flexible substrates to fabricate the photo-FET photodetectors, which exhibit similar performances. The detectivities and the responsivities of the GaSe and GaS[104, 107] can reach 2×10^{14} cm·Hz$^{1/2}$/W and 4 A/W, respectively, in the UV–blue range, as shown in Figure 8(b). For another, GaTe and In_2Se_3[108, 119] with direct bandgap exhibit large responsivities of 1×10^4 A/W at low light illumination power. The response time of these materials ranges from ms to s. Furthermore, the photocurrent has linear property with the excitation power, which indicates that the trap states have an important role in the photoconduction mechanism.

InSe, as a particular case, is a direct bandgap (1.3 eV) when it is bulk. When the thickness of InSe was reduced to 6 nm, it transfers to an indirect bandgap with larger energy[109]. Recently, Tamalampudi *et al.*[120] and Lei *et al.*[121] both studied the performance of 10-nm-thick InSe flakes based photodetectors. Lei and his group reported a 4-layer-thick InSe which have a spectral response to 800 nm wavelengths. The relationship between the wavelength spectra and the photocurrent can fit a parabolic relation, which indicated the indirect bandgap in ultrathin InSe. The response speed of these devices is about 0.5 ms, with a responsivity of 35 mA/W. Moreover, Tamalampudi and his group studied 12 nm thick InSe based photoFETs on both a bendable substrate and an oxidized Si wafer. The responsivities of the device can be tunable by the gate voltage, which can reach up to about 160 A/W. In addition, the response time is about 4 s. Compared with the study of Lei, due to the long lived trap stated which can improve the photoresponse, the device has larger responsivity and longer response time.

In recent years, the layer structures of Sn chalcogenide have also been applied in photodetectors. In particular, SnS_2 has a great attention used in photodetectors and transistors. SnS_2 flakes synthesized by the exfoliating method have been

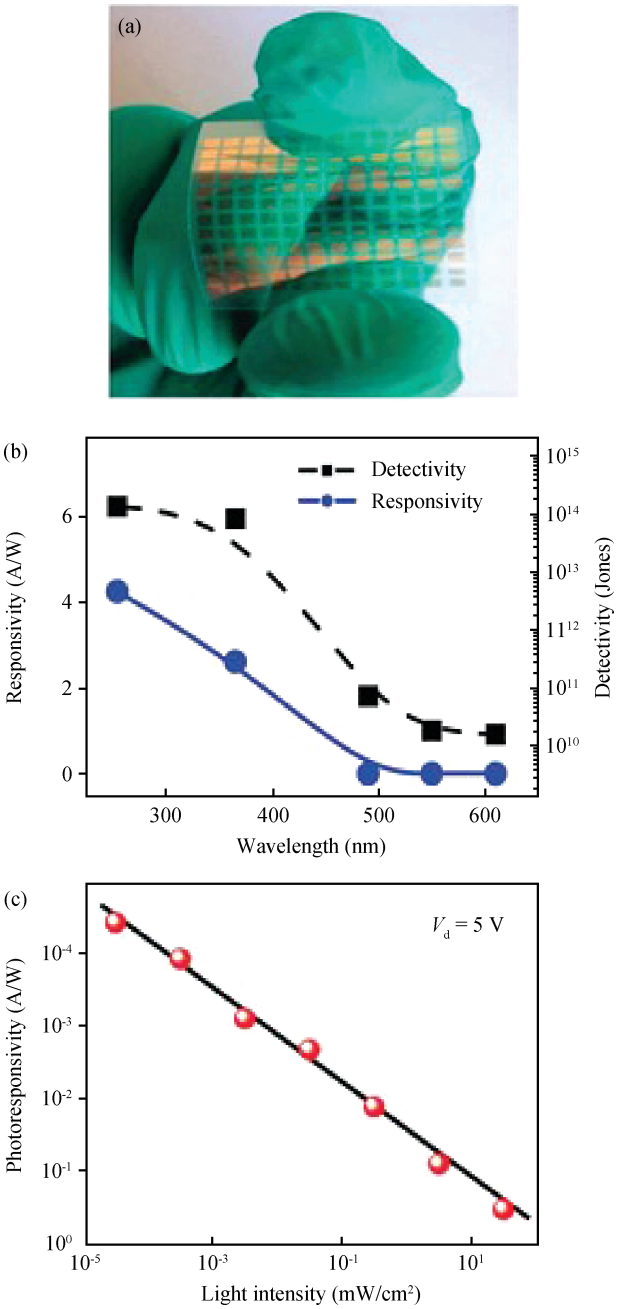

Figure 8. (Color online) (a) Photograph of flexible photodetector based on GaS flakes. (b) Responsivity and detectivity of a GaS photodetector[107]. (c) The function between the responsivity and the excitation power for a GaTe photodetector[109].

investigated in FETs[122]. SnS_2 nanoparticles have already exhibited a good photoresponse[123]. Su and colleagues[124] reported SnS_2 flakes using CVD method and then fabricated for photoFET. The responsivity of the photodetectors based on SnS_2 can be tunable by the gate voltage which can reach up to 8 mA/W with a response time of 5 ms, implying an excellent photoresponse.

Compared with the TMDC based photodetectors, Sn, In and Ga chalcogenides exhibit comparable or larger responsivities. Furthermore, the range of the spectrum response can be extended to the UV region, which has a great potential for application in UV detectors. InSe with thickness reduced below

6 nm, the bandgap can transition from direct-to-indirect, leading to a parabolic absorption with the 1.4 eV photon energy. A large responsivity (160 A/W) and fast response speed (few seconds) have also been found from thicker InSe flakes, which indicates a great influence of trap states. Moreover, SnS_2 based photodetectors have a large responsivity of 8 mA/W and fast response speed, which means that they can be utilized as fast detectors.

6. Summary and outlook

In summary, recent state-of-the-art photodetectors based on 2D layered semiconducting materials have been reviewed. TMDCs based photodetectors, like MoS_2, exhibit high responsivity but slow response speed, which indicate that these materials are more suitable for applications in visible detectors, where the response speed is not very necessary. In addition, MoS_2 also has a large Seebeck coefficient, which means that it could potentially be applied in thermal energy harvesting. The other interesting materials, like GaS, InSe or SnS_2, also exhibit both larger photoresponsivity and faster response speed compared with the MoS_2 based photodetectors, which are promising candidates for sensitive and ultrafast light detection applications. Single-layer WSe_2 with ambipolar transport has been investigated to realize local electrostatic gating controlled electrical devices. Graphene has also exhibited a very fast response and is highly sizeable in photodetection, which means that it has potential application in energy harvesting and optical communications.

To further improve the photoresponse of different 2D materials we could form artificial heterostructures, tailoring the suitable opto-electronic performance for a unique application. For example, graphene/MoS_2 vertical stacks have resulted in ultra-high responsive photodetectors. Besides the photodetector, heterostructures of graphene or TMDCs are good candidates for use in energy harvesting in transparent and flexible solar cells. At present, if we are to optimize device performance, it is necessary to understand the photocurrent and carrier recombination mechanisms. Moreover, for the realization of applications, sizable growth and transfer techniques will be necessary. From the practical point of view, in the measurement environment contact electrodes and device fabrication play the most important factors in the photodetector performance. However, most of the fabrication processes of these devices depend on mechanical exfoliation. CVD-grown materials can offer large-area uniform samples, which is one of the most efficient methods to grow 2D materials. Another challenge is to integrate with the current CMOS technology. So, the CVD growth method may help integrate these 2D materials in CMOS technology.

References

[1] Gu Y, Kwak E S, Lensch J L, et al. Near-field scanning photocurrent microscopy of a nanowire photodetector. Appl Phys Lett, 2005, 87(4): 043111

[2] Tang L, Kocabas S E, Latif S, et al. Nanometre-scale germanium photodetector enhanced by a near-infrared dipole antenna. Nature Photonics, 2008, 2(4): 226

[3] Liu H C, Song C Y, SpringThorpe A J, et al. Terahertz quantum-well photodetector. Appl Phys Lett, 2004, 84(20): 4068

[4] Law J B K, Thong J T L. Simple fabrication of a ZnO nanowire photodetector with a fast photoresponse time. Appl Phys Lett, 2006, 88(13): 133114

[5] Assefa S, Xia F, Vlasov Y A. Reinventing germanium avalanche photodetector for nanophotonic on-chip optical interconnects. Nature, 2010, 464(7285): 80

[6] Butler S Z, Hollen S M, Cao L, et al. Progress, challenges, and opportunities in two-dimensional materials beyond graphene. ACS Nano, 2013, 7(4): 2898

[7] Xu M, Liang T, Shi M, et al. Graphene-like two-dimensional materials. Chem Rev, 2013, 113(5): 3766

[8] Koppens F H L, Mueller T, Avouris P, et al. Photodetectors based on graphene, other two-dimensional materials and hybrid systems. Nature Nanotechnology, 2014, 9(10): 780

[9] Bonaccorso F, Sun Z, Hasan T, et al. Graphene photonics and optoelectronics. Nature photonics, 2010, 4(9): 611

[10] Ferrari A C, Bonaccorso F, Fal'Ko V, et al. Science and technology roadmap for graphene, related two-dimensional crystals, and hybrid systems. Nanoscale, 2015, 7(11): 4598

[11] Sun Z, Hasan T, Torrisi F, et al. Graphene mode-locked ultrafast laser. ACS Nano, 2010, 4(2): 803

[12] Koppens F H L, Chang D E, Garcia de Abajo F J. Graphene plasmonics: a platform for strong light-matter interactions. Nano Lett, 2011, 11(8): 3370

[13] Grigorenko A N, Polini M, Novoselov K S. Graphene plasmonics. Nature Photonics, 2012, 6(11): 749

[14] Kim K S, Zhao Y, Jang H, et al. Large-scale pattern growth of graphene films for stretchable transparent electrodes. Nature, 2009, 457(7230): 706

[15] Pospischil A, Furchi M M, Mueller T. Solar-energy conversion and light emission in an atomic monolayer pn diode. Nature Nanotechnology, 2014, 9(4): 257

[16] Baugher B W H, Churchill H O H, Yang Y, et al. Optoelectronic devices based on electrically tunable pn diodes in a monolayer dichalcogenide. Nature Nanotechnology, 2014, 9(4): 262

[17] Liu M, Yin X, Ulin-Avila E, et al. A graphene-based broadband optical modulator. Nature, 2011, 474(7349): 64

[18] Dawlaty J M, Shivaraman S, Chandrashekhar M, et al. Measurement of ultrafast carrier dynamics in epitaxial graphene. Appl Phys Lett, 2008, 92(4): 042116

[19] Brida D, Tomadin A, Manzoni C, et al. Ultrafast collinear scattering and carrier multiplication in graphene. Nature Communications, 2013, 4

[20] Dawlaty J M, Shivaraman S, Strait J, et al. Measurement of the optical absorption spectra of epitaxial graphene from terahertz to visible. Appl Phys Lett, 2008, 93(13): 131905

[21] Nair R R, Blake P, Grigorenko A N, et al. Fine structure constant defines visual transparency of graphene. Science, 2008, 320(5881): 1308

[22] Kuzmenko A B, Van Heumen E, Carbone F, et al. Universal optical conductance of graphite. Phys Rev Lett, 2008, 100(11): 117401

[23] Li Z Q, Henriksen E A, Jiang Z, et al. Dirac charge dynamics in graphene by infrared spectroscopy. Nature Physics, 2008, 4(7): 532

[24] Wang F, Zhang Y, Tian C, et al. Gate-variable optical transitions in graphene. Science, 2008, 320(5873): 206

[25] Gan X, Shiue R J, Gao Y, et al. Chip-integrated ultrafast graphene photodetector with high responsivity. Nature Photonics, 2013, 7(11): 883

[26] Pospischil A, Humer M, Furchi M M, et al. CMOS-compatible graphene photodetector covering all optical communication bands. Nature Photonics, 2013, 7(11): 892

[27] Wang X, Cheng Z, Xu K, et al. High-responsivity graphene/silicon-heterostructure waveguide photodetectors. Nature Photonics, 2013, 7(11): 888
[28] Novoselov K S, Neto A H C. Two-dimensional crystals-based heterostructures: materials with tailored properties. Physica Scripta, 2012, 2012(T146): 014006
[29] Bonaccorso F, Lombardo A, Hasan T, et al. Production and processing of graphene and 2d crystals. Materials Today, 2012, 15(12): 564
[30] Wilson J A, Yoffe A D. The transition metal dichalcogenides discussion and interpretation of the observed optical, electrical and structural properties. Adv Phys, 1969, 18(73): 193
[31] Castellanos-Gomez A, Poot M, Steele G A, et al. Elastic properties of freely suspended MoS_2 nanosheets. Adv Mater, 2012, 24(6): 772
[32] He K, Poole C, Mak K F, et al. Experimental demonstration of continuous electronic structure tuning via strain in atomically thin MoS_2. Nano Lett, 2013, 13(6): 2931
[33] Conley H J, Wang B, Ziegler J I, et al. Bandgap engineering of strained monolayer and bilayer MoS_2. Nano Lett, 2013, 13(8): 3626
[34] Zhu C R, Wang G, Liu B L, et al. Strain tuning of optical emission energy and polarization in monolayer and bilayer MoS_2. Phys Rev B, 2013, 88(12): 121301
[35] Feng J, Qian X, Huang C W, et al. Strain-engineered artificial atom as a broad-spectrum solar energy funnel. Nature Photonics, 2012, 6(12): 866
[36] Castellanos-Gomez A, Roldán R, Cappelluti E, et al. Local strain engineering in atomically thin MoS_2. Nano Lett, 2013, 13(11): 5361
[37] Britnell L, Ribeiro R M, Eckmann A, et al. Strong light-matter interactions in heterostructures of atomically thin films. Science, 2013, 340(6138): 1311
[38] Buscema M, Island J O, Groenendijk D J, et al. Photocurrent generation with two-dimensional van der Waals semiconductors. Chem Soc Rev, 2015, 44(11): 3691
[39] Rose A. Concepts in photoconductivity and allied problems. Interscience Publishers, 1963
[40] Saleh B E A, Teich M C, Saleh B E. Fundamentals of photonics. New York: Wiley, 1991
[41] Konstantatos G, Sargent E H. Nanostructured materials for photon detection. Nature Nanotechnology, 2010, 5(6): 391
[42] Sze S M, Ng K K. Physics of semiconductor devices. John Wiley & Sons, 2006
[43] Ehrenreich H, Spaepen F. Solid state physic. Academic Press, 2001
[44] Slachter A, Bakker F L, Adam J P, et al. Thermally driven spin injection from a ferromagnet into a non-magnetic metal. Nature Physics, 2010, 6(11): 879
[45] Li Z, Bae M H, Pop E. Substrate-supported thermometry platform for nanomaterials like graphene, nanotubes, and nanowires. Appl Phys Lett, 2014, 105(2): 023107
[46] Wu J, Schmidt H, Amara K K, et al. Large thermoelectricity via variable range hopping in chemical vapor deposition grown single-layer MoS_2. Nano Lett, 2014, 14(5): 2730
[47] Nair R R, Blake P, Grigorenko A N, et al. Fine structure constant defines visual transparency of graphene. Science, 2008, 320(5881): 1308
[48] Mak K F, Ju L, Wang F, et al. Optical spectroscopy of graphene: from the far infrared to the ultraviolet. Solid State Commun, 2012, 152(15): 1341
[49] Xia F, Mueller T, Lin Y, et al. Ultrafast graphene photodetector. Nature Nanotechnology, 2009, 4(12): 839
[50] Mueller T, Xia F, Avouris P. Graphene photodetectors for high-speed optical communications. Nature Photonics, 2010, 4(5): 297
[51] Echtermeyer T J, Britnell L, Jasnos P K, et al. Strong plasmonic enhancement of photovoltage in graphene. Nature Communications, 2011, 2: 458
[52] Shi S F, Xu X, Ralph D C, et al. Plasmon resonance in individual nanogap electrodes studied using graphene nanoconstrictions as photodetectors. Nano Lett, 2011, 11(4): 1814
[53] Liu Y, Cheng R, Liao L, et al. Plasmon resonance enhanced multicolour photodetection by graphene. Nature Communications, 2011, 2: 579
[54] Konstantatos G, Badioli M, Gaudreau L, et al. Hybrid graphene-quantum dot phototransistors with ultrahigh gain. Nature Nanotechnology, 2012, 7(6): 363
[55] Sun Z, Liu Z, Li J, et al. Infrared photodetectors based on CVD-grown graphene and PbS quantum dots with ultrahigh responsivity. Adv Mater, 2012, 24(43): 5878
[56] Engel M, Steiner M, Lombardo A, et al. Light-matter interaction in a microcavity-controlled graphene transistor. Nature Communications, 2012, 3: 906
[57] Gan X, Mak K F, Gao Y, et al. Strong enhancement of light-matter interaction in graphene coupled to a photonic crystal nanocavity. Nano Lett, 2012, 12(11): 5626
[58] Furchi M, Urich A, Pospischil A, et al. Microcavity-integrated graphene photodetector. Nano Lett, 2012, 12(6): 2773
[59] Ferreira A, Peres N M R, Ribeiro R M, et al. Graphene-based photodetector with two cavities. Phys Rev B, 2012, 85(11): 115438
[60] Gan X, Shiue R J, Gao Y, et al. Chip-integrated ultrafast graphene photodetector with high responsivity. Nature Photonics, 2013, 7(11): 883
[61] Wang X, Cheng Z, Xu K, et al. High-responsivity graphene/silicon-heterostructure waveguide photodetectors. Nature Photonics, 2013, 7(11): 888
[62] Zhu X, Yan W, Mortensen N A, et al. Bends and splitters in graphene nanoribbon waveguides. Optics Express, 2013, 21(3): 3486
[63] Kim K, Choi J Y, Kim T, et al. A role for graphene in silicon-based semiconductor devices. Nature, 2011, 479(7373): 338
[64] Youngblood N, Anugrah Y, Ma R, et al. Multifunctional graphene optical modulator and photodetector integrated on silicon waveguides. Nano Lett, 2014, 14(5): 2741
[65] Wang Q H, Kalantar-Zadeh K, Kis A, et al. Electronics and optoelectronics of two-dimensional transition metal dichalcogenides. Nature Nanotechnology, 2012, 7(11): 699
[66] Ayari A, Cobas E, Ogundadegbe O, et al. Realization and electrical characterization of ultrathin crystals of layered transition-metal dichalcogenides. J Appl Phys, 2007, 101(1): 14507
[67] Radisavljevic B, Radenovic A, Brivio J, et al. Single-layer MoS_2 transistors. Nature Nanotechnology, 2011, 6(3): 147
[68] Splendiani A, Sun L, Zhang Y, et al. Emerging photoluminescence in monolayer MoS_2. Nano Lett, 2010, 10(4): 1271
[69] Eda G, Yamaguchi H, Voiry D, et al. Photoluminescence from chemically exfoliated MoS_2. Nano Lett, 2011, 11(12): 5111
[70] Pu J, Yomogida Y, Liu K K, et al. Highly flexible MoS_2 thin-film transistors with ion gel dielectrics. Nano Lett, 2012, 12(8): 4013
[71] He Q, Zeng Z, Yin Z, et al. Fabrication of flexible MoS_2 thin-film transistor arrays for practical gas-sensing applications. Small, 2012, 8(19): 2994
[72] Lee H S, Min S W, Chang Y G, et al. MoS_2 nanosheet phototransistors with thickness-modulated optical energy gap. Nano Lett, 2012, 12(7): 3695
[73] Choi W, Cho M Y, Konar A, et al. High-detectivity multilayer MoS_2 phototransistors with spectral response from ultraviolet to infrared. Adv Mater, 2012, 24(43): 5832
[74] Fontana M, Deppe T, Boyd A K, et al. Electron–hole transport and photovoltaic effect in gated MoS_2 Schottky junctions. Scientific Reports, 2013, 3

[75] Tsai D S, Liu K K, Lien D H, et al. Few-layer MoS_2 with high broadband photogain and fast optical switching for use in harsh environments. ACS Nano, 2013, 7(5): 3905
[76] Wu C C, Jariwala D, Sangwan V K, et al. Elucidating the photoresponse of ultrathin MoS_2 field-effect transistors by scanning photocurrent microscopy. The Journal of Physical Chemistry Letters, 2013, 4(15): 2508
[77] Zhang W, Huang J K, Chen C H, et al. High-gain phototransistors based on a CVD MoS_2 monolayer. Adv Mater, 2013, 25(25): 3456
[78] Yin Z, Li H, Li H, et al. Single-layer MoS_2 phototransistors. ACS Nano, 2011, 6(1): 74
[79] Lopez-Sanchez O, Lembke D, Kayci M, et al. Ultrasensitive photodetectors based on monolayer MoS_2. Nature Nanotechnology, 2013, 8(7): 497
[80] Schedin F, Geim A K, Morozov S V, et al. Detection of individual gas molecules adsorbed on graphene. Nature Materials, 2007, 6(9): 652
[81] Fang H, Chuang S, Chang T C, et al. High-performance single layered WSe_2 p-FETs with chemically doped contacts. Nano Lett, 2012, 12(7): 3788
[82] Late D J, Liu B, Matte H S S R, et al. Hysteresis in single-layer MoS_2 field effect transistors. ACS Nano, 2012, 6(6): 5635
[83] Tongay S, Zhou J, Ataca C, et al. Broad-range modulation of light emission in two-dimensional semiconductors by molecular physisorption gating. Nano Lett, 2013, 13(6): 2831
[84] Perea-López N, Lin Z, Pradhan N R, et al. CVD-grown monolayered MoS_2 as an effective photosensor operating at low-voltage. 2D Materials, 2014, 1(1): 011004
[85] Furchi M M, Polyushkin D K, Pospischil A, et al. Mechanisms of photoconductivity in atomically thin MoS_2. Nano Lett, 2014, 14(11): 6165
[86] Tsai D S, Lien D H, Tsai M L, et al. Trilayered MoS metal–semiconductor–metal photodetectors: photogain and radiation resistance. IEEE Journal of Selected Topics in Quantum Electronics, 2014, 20(1): 30
[87] Boscher N D, Carmalt C J, Palgrave R G, et al. Atmospheric pressure CVD of molybdenum diselenide films on glass. Chemical Vapor Deposition, 2006, 12(11): 692
[88] Chang Y H, Zhang W, Zhu Y, et al. Monolayer $MoSe_2$ grown by chemical vapor deposition for fast photodetection. ACS Nano, 2014, 8(8): 8582
[89] Lu X, Utama M I B, Lin J, et al. Large-area synthesis of monolayer and few-layer $MoSe_2$ films on SiO_2 substrates. Nano Lett, 2014, 14(5): 2419
[90] Shaw J C, Zhou H, Chen Y, et al. Chemical vapor deposition growth of monolayer $MoSe_2$ nanosheets. Nano Res, 2014, 7(4): 511
[91] Shim G W, Yoo K, Seo S B, et al. Large-area single-layer $MoSe_2$ and its van der Waals heterostructures. ACS Nano, 2014, 8(7): 6655
[92] Xia J, Huang X, Liu L Z, et al. CVD synthesis of large-area, highly crystalline $MoSe_2$ atomic layers on diverse substrates and application to photodetectors. Nanoscale, 2014, 6(15): 8949
[93] Abderrahmane A, Ko P J, Thu T V, et al. High photosensitivity few-layered $MoSe_2$ back-gated field-effect phototransistors. Nanotechnology, 2014, 25(36): 365202
[94] Perea-López N, Elías A L, Berkdemir A, et al. Photosensor device based on few-layered WS_2 films. Advanced Functional Materials, 2013, 23(44): 5511
[95] Huo N, Yang S, Wei Z, et al. Photoresponsive and gas sensing field-effect transistors based on multilayer WS_2 nanoflakes. Scientific Reports, 2014, 4: 5209
[96] Zhang W, Chiu M H, Chen C H, et al. Role of metal contacts in high-performance phototransistors based on WSe_2 monolayers. ACS Nano, 2014, 8(8): 8653
[97] Podzorov V, Gershenson M E, Kloc C, et al. High-mobility field-effect transistors based on transition metal dichalcogenides. Appl Phys Lett, 2004, 84(17): 3301
[98] Das S, Appenzeller J. WSe_2 field effect transistors with enhanced ambipolar characteristics. Appl Phys Lett, 2013, 103(10): 103501
[99] Huang J K, Pu J, Hsu C L, et al. Large-area synthesis of highly crystalline WSe_2 monolayers and device applications. ACS Nano, 2013, 8(1): 923
[100] Ross J S, Klement P, Jones A M, et al. Electrically tunable excitonic light-emitting diodes based on monolayer WSe_2 pn junctions. Nature Nanotechnology, 2014, 9(4): 268
[101] Groenendijk D J, Buscema M, Steele G A, et al. Photovoltaic and photothermoelectric effect in a double-gated WSe_2 device. Nano Lett, 2014, 14(10): 5846
[102] Baugher B W H, Churchill H O H, Yang Y, et al. Optoelectronic devices based on electrically tunable pn diodes in a monolayer dichalcogenide. Nature Nanotechnology, 2014, 9(4): 262
[103] Pospischil A, Furchi M M, Mueller T. Solar-energy conversion and light emission in an atomic monolayer pn diode. Nature Nanotechnology, 2014, 9(4): 257
[104] Hu P A, Wen Z, Wang L, et al. Synthesis of few-layer GaSe nanosheets for high performance photodetectors. ACS Nano, 2012, 6(7): 5988
[105] Late D J, Liu B, Luo J, et al. GaS and GaSe ultrathin layer transistors. Adv Mater, 2012, 24(26): 3549
[106] Liu H, Peide D Y. Dual-gate MOSFET with atomic-layer-deposited as top-gate dielectric. IEEE Electron Device Lett, 2012, 33(4): 546
[107] Hu P A, Wang L, Yoon M, et al. Highly responsive ultrathin GaS nanosheet photodetectors on rigid and flexible substrates. Nano Lett, 2013, 13(4): 1649
[108] Jacobs-Gedrim R B, Shanmugam M, Jain N, et al. Extraordinary photoresponse in two-dimensional In_2Se_3 nanosheets. ACS Nano, 2013, 8(1): 514
[109] Mudd G W, Svatek S A, Ren T, et al. Tuning the bandgap of exfoliated InSe nanosheets by quantum confinement. Adv Mater, 2013, 25(40): 5714
[110] Capozzi V, Montagna M. Optical spectroscopy of extrinsic recombinations in gallium selenide. Phys Rev B, 1989, 40(5): 3182
[111] Alekperov O Z, Godjaev M O, Zarbaliev M Z, et al. Interband photoconductivity in layer semiconductors GaSe, InSe and GaS. Solid State Commun, 1991, 77(1): 65
[112] Genut M, Margulis L, Hodes G, et al. Preparation and microstructure WS_2 thin films. Thin Solid Films, 1992, 217(1): 91
[113] Plucinski L, Johnson R L, Kowalski B J, et al. Electronic band structure of GaSe (0001): angle-resolved photoemission and ab initio theory. Phys Rev B, 2003, 68(12): 125304
[114] Ho C H, Lin S L. Optical properties of the interband transitions of layered gallium sulfide. J Appl Phys, 2006, 100(8): 3508
[115] Sánchez-Royo J F, Pellicer-Porres J, Segura A, et al. Angle-resolved photoemission study and first-principles calculation of the electronic structure of GaTe. Phys Rev B, 2002, 65(11): 115201
[116] De Groot C H, Moodera J S. Growth and characterization of a novel In_2Se_3 structure. J Appl Phys, 2001, 89(8): 4336
[117] Sánchez-Royo J F, Segura A, Lang O, et al. Optical and photovoltaic properties of indium selenide thin films prepared by van der Waals epitaxy. J Appl Phys, 2001, 90(6): 2818
[118] Sreekumar R, Jayakrishnan R, Kartha C S, et al. Enhancement of band gap and photoconductivity in gamma indium selenide due to swift heavy ion irradiation. J Appl Phys, 2008, 103(2): 023709
[119] Liu F, Shimotani H, Shang H, et al. High-sensitivity photodetectors based on multilayer GaTe flakes. ACS Nano, 2014, 8(1):

752
[120] Tamalampudi S R, Lu Y Y, Kumar U R, et al. High performance and bendable few-layered InSe photodetectors with broad spectral response. Nano Lett, 2014, 14(5): 2800
[121] Lei S, Ge L, Najmaei S, et al. Evolution of the electronic band structure and efficient photo-detection in atomic layers of InSe. ACS Nano, 2014, 8(2): 1263
[122] De D, Manongdo J, See S, et al. High on/off ratio field effect transistors based on exfoliated crystalline SnS_2 nano-membranes. Nanotechnology, 2012, 24(2): 025202
[123] Tao Y, Wu X, Wang W, et al. Flexible photodetector from ultraviolet to near infrared based on a SnS_2 nanosheet microsphere film. Journal of Materials Chemistry C, 2015, 3(6): 1347
[124] Su G, Hadjiev V G, Loya P E, et al. Chemical vapor deposition of thin crystals of layered semiconductor SnS_2 for fast photodetection application. Nano Lett, 2014, 15(1): 506